IVYSPRING INTERNATIONAL PUBLISHER

Theranostics

2017; 7(10): 2690-2703. doi: 10.7150/thno.18914

Research Paper

Therapeutic Effect of Astroglia-like Mesenchymal Stem Cells Expressing Glutamate Transporter in a Genetic Rat Model of Depression

Amit Shwartz[1], Oshra Betzer[2, 3], Noam Kronfeld[1], Gila Kazimirsky[1], Simona Cazacu[4], Susan Finniss[4], Hae Kyung Lee[4], Menachem Motiei[2], Shani Yael Dagan[1], Rachela Popovtzer[2], Chaya Brodie[1, 4]✉, Gal Yadid[1, 3]✉

1. The Mina & Everard Goodman Faculty of Life Sciences, Bar-Ilan University, Ramat-Gan 52900, Israel;
2. Faculty of Engineering and the Institute of Nanotechnology and Advanced Materials, Bar-Ilan University, Ramat Gan 5290002, Israel;
3. Leslie Susan Gonda (Goldschmied) Multidisciplinary Brain Research Center, Bar-Ilan University, Ramat Gan 52900, Israel;
4. Hermelin Brain Tumor Center, Henry Ford Hospital, Detroit, MI, USA 48202.

✉ Corresponding authors: **Prof. Gal Yadid,** The Mina & Everard Goodman Faculty of Life Sciences, Leslie Susan Gonda (Goldschmied) Multidisciplinary Brain Research Center; Bar-Ilan University, Ramat-Gan 5290002, Israel Tel: 972-3-5318123 E-mail: yadidg@gmail.com **Chaya Brodie,** The Mina & Everard Goodman Faculty of Life Sciences, Leslie Susan Gonda (Goldschmied) Multidisciplinary Brain Research Center; Bar-Ilan University, Ramat-Gan 5290002, Israel Email: chaya@brodienet.com

Received: 2016.10.25; Accepted: 2017.02.15; Published: 2017.07.06

Abstract

Recent studies have proposed that abnormal glutamatergic neurotransmission and glial pathology play an important role in the etiology and manifestation of depression. It was postulated that restoration of normal glutamatergic transmission, by enhancing glutamate uptake, may have a beneficial effect on depression. We examined this hypothesis using unique human glial-like mesenchymal stem cells (MSCs), which in addition to inherent properties of migration to regions of injury and secretion of neurotrophic factors, were differentiated to express high levels of functional glutamate transporters (excitatory amino acid transporters; EAAT). Additionally, gold nanoparticles (GNPs), which serve as contrast agents for CT imaging, were loaded into the cells for non-invasive, real-time imaging and tracking of MSC migration and final location within the brain. MSC-EAAT (2×10^5; 10 µl) were administered (i.c.v.) to Flinder Sensitive Line rats (FSLs), a genetic model for depression, and longitudinal behavioral and molecular changes were monitored. FSL rats treated with MSC-EAAT showed attenuated depressive-like behaviors (measured by the forced swim test, novelty exploration test and sucrose self-administration paradigm), as compared to controls. CT imaging, Flame Atomic Absorption Spectroscopy analysis and immunohistochemistry showed that the majority of MSCs homed specifically to the dentate gyrus of the hippocampus, a region showing structural brain changes in depression, including loss of glial cells. mRNA and protein levels of EAAT1 and BDNF were significantly elevated in the hippocampus of MSC-EAAT-treated FSLs. Our findings indicate that MSC-EAATs effectively improve depressive-like manifestations, possibly in part by increasing both glutamate uptake and neurotropic factor secretion in the hippocampus.

Introduction

Depression is a disabling and complex psychiatric disease, causing extensive impairments in daily functioning and an overall deterioration in quality of life [1]. Most existing antidepressants modulate monoamine transmission, yet many patients experience low remission rates and residual symptoms [2].

Recent studies suggest that not only the monoaminergic system, but also glutamatergic abnormalities and glial pathology play a significant role in the etiology and manifestation of depression [2]. In individuals with mood disorders and in suicide

victims, changes in glutamate levels were observed in plasma [3], serum [2, 4, 5], cerebrospinal fluid [6] and brain tissue [7-9]. Glutamatergic impairments are also found in animal models of depression, including the genetic rat model for depression, Flinders Sensitive Line (FSL). FSL rats show increased resting glutamate levels and glutamate transients in the prefrontal cortex [10], and in the hippocampus, defective group-2 [11] and reduced group-5 [12] metabotropic glutamate receptors, and lower synaptic expression of NR1 subunit of the NMDA receptor are found [13]. A consistent neuropathological finding in major depressive disorder is the reduction in the number of glia [14-19], which can decrease neural plasticity. FSLs show dysfunctional astrocytic regulation of glutamate transmission in the hippocampus [14], including down-regulation of glial excitatory amino acid transporter (EAAT) 1, a key member of the glutamate/neutral amino acid transporter protein family [14]. Recent post-mortem genome-wide analyses of depressed individuals have shown significant changes in expression clusters of glutamate signaling genes, glia-associated genes and growth factor genes that indicate impairment of the glutamate reuptake mechanism in specific cortical regions [20, 21]. Specifically, the analyses show down-regulation of high-affinity glial EAAT1 and 2, and decreased expression of glutamine synthetase, which converts glutamate to nontoxic glutamine. These changes could produce elevated extracellular glutamate levels, which not only affects signaling, but also has potential neurotoxic effects. In addition, NMDARs regulate dendritic branching [22], and excessive glutamatergic transmission, via exposure to chronic stress, causes dendritic retraction and loss of spines [23], while antidepressants of various classes were suggested to trigger dendritic remodeling and synaptic plasticity in the hippocampus and prefrontal cortex [24]. Various glutamatergic agents have been suggested as possible antidepressants [2, 25-31], although sedative and psychotomimetic side effects may limit use of some of these agents.

Herein, we differentiated human glial-like mesenchymal stem cells (MSCs) to express high levels of functional EAAT1 and EAAT2 by treating the MSCs with altered medium components and concentrations. To the best of our knowledge, this novel development has not been achieved by others (see Methods). After verifying EAAT expression and the functionality of the differentiated cells, we then examined these unique cells as a means for alleviating depressive-like behavior. Stem cell-based therapy using MSCs is being explored in a large number of clinical trials, including for possible treatment of brain pathologies [32-37]. MSCs home to sites of injury and inflammation [38, 39], secreting anti-inflammatory and neurotrophic factors therein [39, 40]. Additionally, MSCs can promote endogenous neurogenesis [41] and differentiate into neural-like cell types [42, 43]. A critical problem for development and implementation of stem cell-based therapy is the lack of reliable, non-invasive means to trace and image the cells within deep brain structures [44-47]. Cell therapy for neurological disorders is more challenging than for internal disorders, which can be evaluated with comparatively objective measures and markers [48, 49]. Consistent and unbiased *in viv*o data, such as migration and bio-distribution patterns is lacking [50, 51]. These obstacles can be overcome by quantitative imaging techniques such as CT, using gold nanoparticles (GNPs) as powerful contrast agents [45, 47, 50-53]. We have recently provided a solution for the challenge and need for a reliable GNP uploading protocol, which on the one hand, provides sufficient nanoparticle uploading to achieve maximum visibility of cells, and on the other hand, assures a minimal effect of particles on cell function and viability. Our optimized protocol for nanoparticle-cell labeling show that GNPs penetrate and accumulate within stem cells, without impairing cell viability, proliferation and functionality [54]. Thus, GNPs can be safely used for labeling and real-time, prolonged tracking of cells. We have also recently shown that GNP-loaded MSCs are a safe, non-invasive means for long-term, *in-vivo* CT imaging and tracking, providing real-time information on cell homing, up to four weeks post-transplantation in rat brain [44-47, 55].

Herein, MSCs expressing EAAT (MSC-EAAT), labeled with GNPs, were injected intracerebroventricularly (i.c.v) to FSL rats, and behavioral and molecular changes were monitored longitudinally, in addition to real-time CT tracking of the migration path and final location of the cells within the brain.

Materials and Methods

Glia-like differentiation of MSCs

Human undifferentiated adipose tissue-derived MSCs (ScienCell Research Laboratories, CA) were propagated and maintained in DMEM with FBS (10%), gentamicin (50 µg/ml), nonessential amino acid (5mM) and glutamine (5mM) (37°C, 5% CO_2 humidified atmosphere). For glia-like differentiation, MSCs were treated with DMEM/Opti-MEM with F12 – B 27.5%, FGFb (50ng/ml), SHH (250ng/ml) and EGF (50ng/ml), for 3 weeks (37°C, 5% CO_2). Patent pending for full differentiation process.

GNP synthesis and characterization

Spherical GNPs (20nm) were synthesized using sodium citrate as a reducing agent, based on a well-established procedure [54, 56]. GNPs were conjugated to MDDA linker (12-mercaptododecanoic acid, Sigma) then coated with D-(þ)-glucosamine hydrochloride (Sigma), due to its stability and high cell-uptake rate.

GNP labeling of cells

D-(+)-Glucosamine hydrochloride (3mg) was added to activated linker-coated GNPs (30 µg/ml), added in excess to MSCs (one million particles/cell), and incubated (37°C, 3 hours). GNPs undergo endocytosis [37, 57] through a receptor-mediated endocytosis internalization mechanism [58]. Medium was washed twice with PBS, then treated with trypsin; cells were centrifuged twice (7 min, 1000 rpm) to wash out unbound nanoparticles. GNP uptake (measured by Flame Atomic Absorption Spectroscopy (FAAS; below) was $1.1\times10^6 \pm 0.12$ per cell.

Real-time quantitative PCR analysis

Total EAAT1 and EAAT2 RNA was isolated from cultured MSCs in astrocytic or control mediums using QIAzol reagent (Qiagen, CA). 0.5µg of RNA was used to synthesize cDNA by Thermoscript (Invitrogen) with oligo dT primers, followed by SYBR green qPCR method (primers and further details in Supplementary Information (SI)).

Western blot analysis

Cell lysates from control and differentiated MSCs (30µg protein) were resolved by SDS-PAGE and transferred to nitrocellulose membranes. Rabbit anti-EAAT1 and EAAT2 antibodies (Santa Cruz Biotechnology, USA)) and goat anti-actin antibody (Sigma, USA) were used. Following incubation with the primary and secondary antibodies, immunoreactive bands were visualized by ECL Western blotting detection kit (Amersham, USA).

MSCs [^{3}H]glutamate uptake

Cells were plated at 2.0×10^5 cells per well, washed twice in DMEM, transferred to Krebs buffer (1h, 37°C), then incubated with 1 ml L-[3,4-3H]glutamate for 10, 60 and 90 min. Uptake was terminated by ice-cold PBS (3ml). [^{3}H]-Glutamate levels were determined with liquid scintillation counter.

MTT cell proliferation assay

Cells were plated (100,000/well, 24-well plate) and GNP solution (500µL) was added to each well. Controls received fresh media only. After 48 hrs, GNP solution was replaced with mixture of 400µL media and 40µL of MTT powder at 5mg/mL in PBS. Two hours later, media was aspirated and 1mL of DMSO was added to each well. 50µL was immediately transferred to a 96-well plate and absorbance was measured at 560nm.

Animals

Adult male FSL and Sprague-Dawley (SD) rats (>230g) were maintained under conditions of unvarying temperature (23°C) and humidity (50%), in a 12:12h light/dark cycle and with free access to food and water, as approved by the Animal Care Committee of Bar-Ilan University and in accordance with the NIH Guide for the Care and Use of Laboratory Animals.

MSC treatment

FSL and SD rats were habituated to the animal housing room for 1 week. Baseline behavioral measurements (detailed below and in SI) were conducted. Twenty-four hours later, animals were anesthetized with ketamine hydrochloride (100mg/kg, i.p.) and xylazine (10mg/kg, i.p.), then placed in a stereotaxic apparatus (David Kopf). A hole was drilled through the skull and a 10µl Hamilton syringe was inserted unilaterally into the left lateral ventricle (anterior −0.8, lateral 1.5, ventral -4.0mm from the bregma).

FSL rats received either $2x10^5$ MSC-EAAT or undifferentiated MSCs labeled with GNPs (total volume 10µl; n=10 or n=6, respectively), or vehicle with free GNPs as control (10µl; 30mg/mL; n=10). SD rats (n=7) received vehicle. Naïve FSLs (n=7) were included as additional control in the behavioral tests. Injection rate was 2µl/min, over 5 min. Antibiotics (Baytril, 0.4ml, s.c.) and analgesics (Rimadyl, 0.05ml, s.c.) were administrated for 3 consecutive days.

All behavioral tests were measured and analyzed using Noldus Ethovision 7.0 XT camera and video tracking software package. A camera placed above the open field recorded behavior. Video and computer equipment were situated in a separate room.

A timeline of *in vivo* experiments is presented in Fig. 1.

Locomotor Activity Test

Tests were conducted 24 hours before injections, and on day 19 after treatment. Rats (n=7 from each group, in this and in subsequent behavioral tests) were placed in a plastic polymer box (60×60×30 cm), for 5 minutes. Total mobility time and average velocity of each animal were calculated.

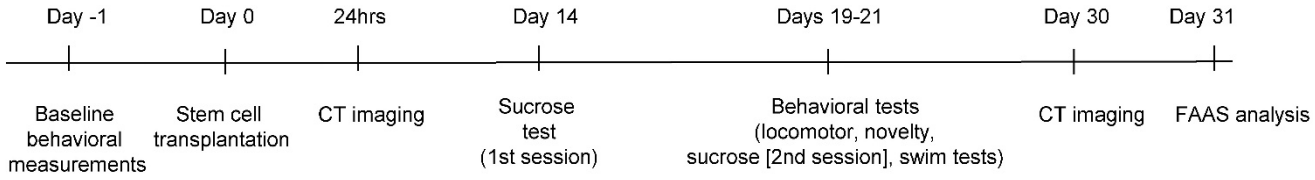

Figure 1. Timeline of *in vivo* experiments

Novelty Exploration Test

Tests were conducted 24 hours before injections, and on day 20 after treatment. Rats were allowed to explore a new object for 5 min in a plastic polymer box (60×60×30 cm). The object, with a complex texture surface (glass ball, 15×6×5 cm) was placed in the center of the exploration area. Total duration of time spent exploring the object was recorded [59, 60].

Sucrose self-administration

Tests (as in [61] and detailed in SI) were conducted 24 hours before injections, and on days 14, 20 after treatment. Briefly, to test whether treatment increases basic reward behavior ('anhedonia', a measure of depressive-like behavior [62, 63]), rats were transferred daily into operant conditioning chambers (30 min), during their dark cycle, and allowed to self-administer sucrose (10% sucrose solution; 0.13ml per infusion) delivered into a liquid drop receptacle upon pressing on the active lever. Animals had free access to water and food, ensuring that the test measured only anhedonic behavior.

Forced Swim Test

Depressive-like behavior (despair) was measured on day 21, by time of immobility (suspension of swimming, so that both hind paws were immobile) in the modified version of the Porsolt Forced Swim Test [61], over 5 min. Rats were placed in a cylindrical tank (40cm height X 18cm diameter) with water (rat could not touch the bottom with its hind paws). As the model is genetic, this test does not serve to induce depressive-like behavior but to examine efficacy of treatment on behavior.

In-vivo micro-CT scans

Animals (n=3 for treated FSLs and free-GNP injected FSLs) were scanned in-vivo with a micro-CT scanner (Skyscan High Resolution Model 1176, Bruker micro-CT, Kontich, Belgium; nominal resolution of 35µm, a 0.5 mm aluminum filter, and applied x-ray tube voltage of 45 kV; detection limit ~1000 GNP-labeled cells), to screen for the location of the cells one day and one month after injection. Specifications and further details in SI. At the end of the experiment, brains where taken for further ex-vivo scans and FAAS analysis.

Ex-vivo micro-CT scans

Brains were removed and placed in 10% buffered formalin for 5 days of fixation, then soaked in lopamidol (150mg/ml), diluted with 7.5% paraformaldehyde at 4°C for 14 days. Brains were scanned with micro-CT at nominal resolution of 9µm, with aluminum filter 0.2mm thick and an applied x-ray tube voltage of 45 kV, camera pixel binning of 2×2, scan orbit 180 with rotation step of 0.4°. An additional contrast agent was used for *ex vivo* scans, due to minimal differences in density and X-ray absorption between different brain tissue types (i.e., no native CT contrast). A procedure based on previous studies (de Crespigny *et al.* [64], Saito [65]) was used and modified in order to be applied to rat brains, further detailed in SI.

FAAS analysis

FAAS (SpectrAA 140, Agilent Technologies) was used to determine amounts of gold in each region, and thus quantify the exact amount of cells that reached each brain region. Punches from 30 different brain regions were taken using a stainless steel cannula with an inner diameter of 1.1 mm; among the main regions taken and examined were the prefrontal cortex, nucleus accumbens, central amygdala, basolateral amygdala, ventral tegmental area, dentate gyrus, bed nucleus of stria terminalis, substantia nigra, lateral habenula, cingulate cortex, striatum, arcuate nucleus and ventricles. The punches were melted with aqua regia acid, evaporated, filtered and diluted to 5 ml. Gold concentration was determined with Au lamp according to the absorbance value with correlation to the calibration curve with known gold concentrations (commonly: 0.1, 1, 2 and, 5mg/ml). Amount of cells/region was calculated by amount of gold per region divided by number of GNPs uptaken into the cells (see *GNP labeling* section and [55]).

Immunohistochemistry

After conclusion of the behavioral tests (day 21), brains were removed (n=2) and post-fixed. Tissues were cryosectioned (30µm, coronal plane), 10 slices/brain were washed in PBS, treated with blocking solution (1h) and then incubated overnight

with primary antibodies (monoclonal mouse anti-human mitochondria, monoclonal rabbit anti-human/mouse/rat BDNF, polyclonal rabbit anti-human/mouse/rat EAAT1). Slices were incubated with secondary antibodies (1h) (goat anti-mouse (mitochondria), goat anti-rabbit (EAAT1), goat anti-rabbit (BDNF)), and with DAPI solution (0.0005mg/ml, 2 min) to visualize cell nuclei. For control, slices were not incubated with primary antibody (further detailed in SI).

Real-time quantitative PCR of EAAT and BDNF brain

On day 21 brains were removed and bi-hemispheric hippocampal brain punches were taken. Total RNA, cDNA and TaqMan stem-loop RT-qPCR for expression of human EAAT1 and rat BDNF were determined as detailed above and in SI.

Statistical Analysis

For behavioral tests, one-way ANOVA or two-way ANOVA with repeated measures followed by Bonferroni's multiple comparison or Tukey's post hoc was performed. Differences between two groups were analyzed using Student's t-test.

Results

Characterization of differentiated MSCs and GNP labeling

Differentiated MSCs were assessed for mRNA expression and protein levels of glutamate transporters using RT-qPCR and western blot analysis. We found significantly higher mRNA expression levels of EAAT1 and EAAT2 in differentiated, as compared to control undifferentiated, MSCs (Student's t-test; $p<0.0001$) (Figure 2a). Western blot detected EAAT1 and EAAT2 proteins expressed in differentiated, and not in control undifferentiated, MSCs (Figure 2b). Functionality of MSC-EAAT was determined by a glutamate uptake assay, showing a time-dependent increase in glutamate uptake into these cells ($p < 0.001$; Figure 2c).

MSC-EAATs and undifferentiated MSCs were loaded with GNPs. The average amount of gold nanoparticle uptake, analyzed using FAAS, was 1.1 million (std: 0.12) per cell, showing efficient labeling of the cells. Viability, metabolism and proliferation of MSC-EAATs was not altered after labeling with GNPs as compared to control cells without GNPs, as assessed at several time points over an eight-day period using an MTT cell proliferation assay (data not shown).

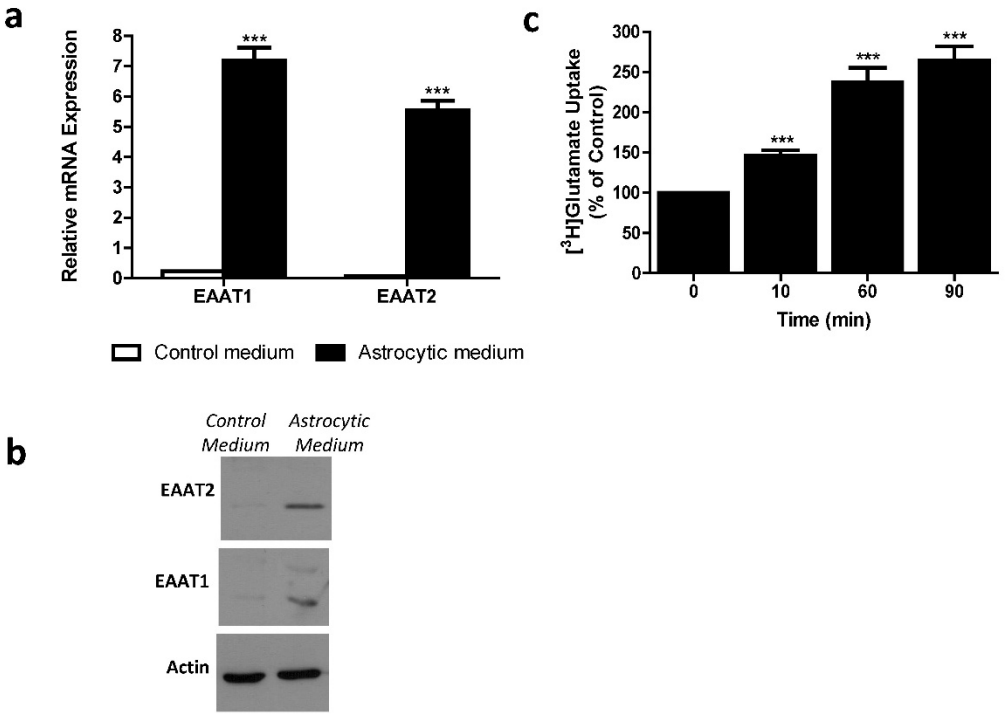

Figure 2. Astrocytic profiling of MSCs. a. EAAT1 and EAAT2 mRNA expression levels. Both EAAT1 and EAAT2 mRNA expression levels were significantly higher in cells treated with astrocytic medium compared to negligible levels in cells treated with control medium. Results expressed in arbitrary units. (***p<0.001). **b.** EAAT1 and EAAT2 protein levels. Immunoreactive EAAT1 and EAAT2 bands from cell lysates of MSCs cultured with astrocytic or control mediums are shown. Bands are seen only in cells cultured with astrocytic medium. **C.** Glutamate uptake assay. [3H]Glutamate uptake was measured in control and differentiated MSCs from adipose origin. Data presented as percentage of glutamate uptake of differentiated MSCs from undifferentiated (control) MSCs at 3 time points post incubation with [3H]glutamate. The results of panels a, b and c are the means ± SEM of three different experiments. (***p<0.001).

Effect of MSC-EAAT on depressive-like behavior

We next examined the long-term effect of treatment with MSC-EAAT (n=10) on depressive-like behaviors of FSL rats as compared to FSLs treated with undifferentiated MSCs (n=6), naive FSLs (n=7), free GNP-treated FSLs (n=10), and SD rats (n=7). In the locomotor activity test on day 19 no significant differences were found in total distance moved or average velocity between all treatment and control groups (distance moved (M): 15±2 control, 14±2 MSC-EAAT-treated FSLs, 12±3 undifferentiated MSC-treated FSLs; velocity (cm/sec): 6±2 control, 5±1 MSC-EAAT-treated FSLs, 4±2 undifferentiated MSC-treated FSLs, one-way ANOVA, $p>0.05$).

In the novelty exploration test on day 20 (Figure 3a), a one-way ANOVA followed by Bonferroni's multiple comparison post hoc test showed that time spent exploring a new object was significantly longer in MSC-EAAT-treated FSLs, as compared to naïve FSLs and free GNP-treated FSLs, and in SD rats as compared to undifferentiated MSC-treated FSLs, naïve FSLs and free GNP-treated FSLs (one-way ANOVA $F(4, 30)=11.44$, $p<0.0001$; post hoc: MSC-EAAT-treated FSLs vs. naive FSLs and GNP-treated FSLs, $p<0.05$; SD vs. naive FSLs and free GNP-treated FSLs, $p<0001$; SD vs. undifferentiated MSC-treated FSLs, $p<0.001$).

In the forced swim test, rats that received differentiated MSC-EAAT showed a significant decrease in percentage of immobility time from baseline during the swim test on day 21, as compared to undifferentiated MSC-treated, naïve, or free GNP-treated FSLs, and SD rats (one-way ANOVA $F(4, 25)=8.56$, $p<0.001$; followed by Bonferroni's multiple comparison post-hoc test; naive FSL vs. MSC-EAAT-treated FSLs $p<0.0001$; FSL GNP vs MSC-EAAT-treated FSLs, $p<0.001$; SD vs MSC-EAAT-treated FSL, $p<0.0001$; undifferentiated MSC-treated FSL vs. MSC-EAAT-treated FSLs, $p<0.05$) (Figure 3b).

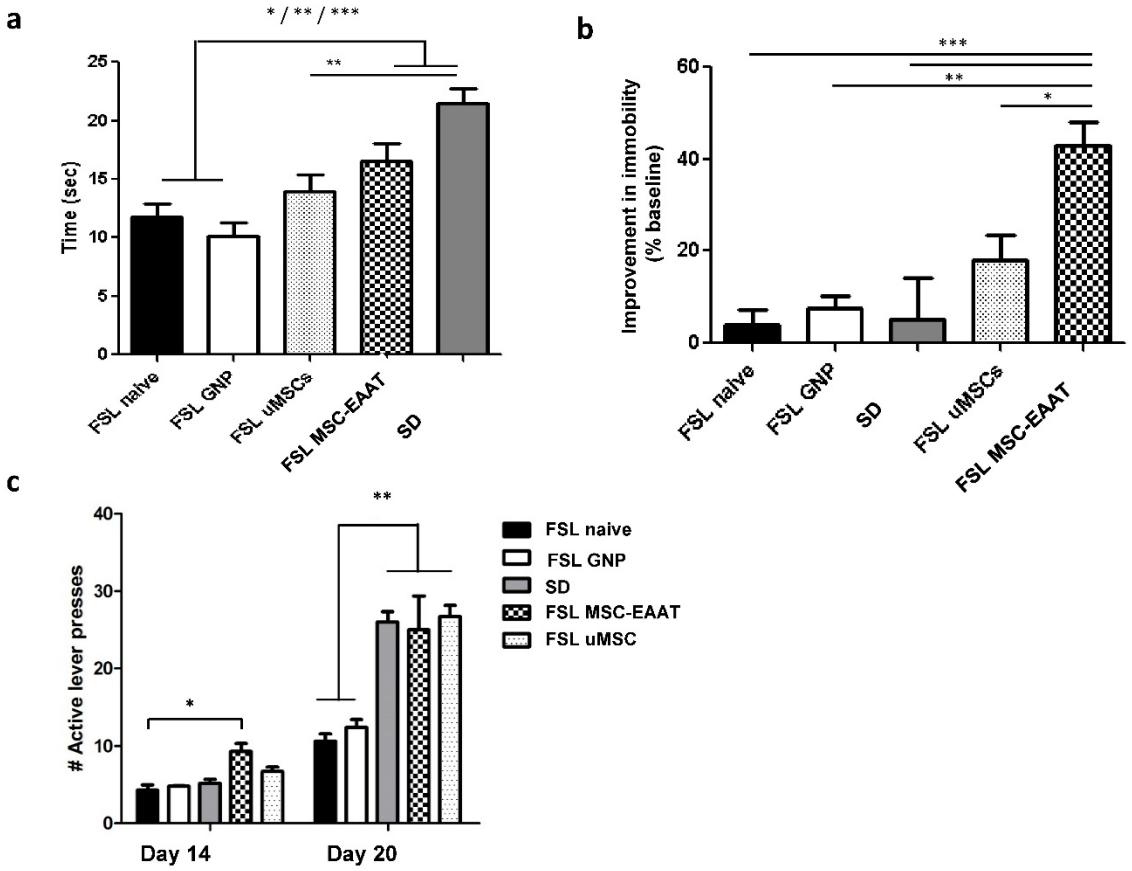

Figure 3. Effect of MSC-EAAT on depressive-like manifestations. a. Novelty exploration test. Rats that received MSC-EAATs (n=10) and SD controls (n=7) spent a significantly longer amount of time exploring a novel object vs. naïve FSLs (n=7), GNP-treated FSLs (n=10), and undifferentiated MSC ('uMSC')-treated FSLs (n=6) (one-way ANOVA, MSC-EAAT-treated FSLs vs naive FSLs *p<0.05; SD vs naive FSLs, ***p<0001; MSC-EAAT-treated FSLs vs free GNP-treated FSLs, *p<0.05; SD vs GNP-treated FSLs, ***p<0.0001; SD vs undifferentiated MSC-treated FSLs, **p<0.001). Values presented as mean ± SEM. **b.** Forced swim test. Rats that received MSC-EAAT showed a significant decrease in immobility time during the swim test as compared to (one-way ANOVA followed by Bonferroni's multiple comparison post-hoc; MSC-EAAT-treated FSLs vs. naive FSLs ***p<0.0001; MSC-EAAT-treated FSLs vs. GNP-treated FSLs, **p<0.001; MSC-EAAT-treated FSLs vs. SD, ***p<0.0001; MSC-EAAT-treated FSLs vs. undifferentiated MSC-treated FSLs, *p<0.05). **c.** FSLs treated with MSC-EAAT or undifferentiated cells, and SD rats, show higher hedonia compared to naïve FSLs and free GNP-treated FSLs (day 1: MSC-EAAT-treated FSLs vs. naive FSLs *p<0.05; day 7: MSC-EAAT-treated FSLs, undifferentiated MSC-treated FSLs and SD vs. naive FSLs and GNP-treated FSLs, **p<0.001).

Previous findings have shown that treatment of mice with acute ketamine (30 mg/kg, though a higher dose did not have an effect) given one week before, though not after, social defeat-induced depression, lowered immobility in the swim test [66]. Therefore, to rule out a confounding effect, we examined the effect of the anesthesia (a single injection of ketamine hydrochloride (100 mg/kg, i.p.; before surgery)) on immobility in the swim test, in a new group of FSL rats (n=3) at baseline, and then 24hrs, 3 days, 4 days, 7 days and 12 days after surgery. We found a significant decrease in immobility as compared to baseline 24 hrs after ketamine injection, which then increased back to pre-treatment levels on day three after treatment, and persisted up to day 12 (baseline: 238±13.9 sec; 24 hrs after injection: 190.33±12.07 sec; days 3,4,7,12 after treatment: 263.66±4.9, 274.33±6.01, 251.66±8.83, and 267.66±3.56 sec, respectively; one-way ANOVA with repeated measures: $F(95,170)=3.7$, $p<0.04$; Tukey's post hoc, $p<0.05$ for day 1 only vs. baseline; n=3).

Anhedonia was measured using a sucrose self-administration test. A two-way ANOVA with repeated measures showed a main effect of group ($F(4, 46)=24.45$, $p<0.0001$), main efect of time ($F(1, 46)=276.7$, $p<0.0001$), and interaction between group and time ($F(4, 46)=12.93$, $p<0.0001$). A Bonferroni post-hoc test showed higher hedonic-like behavior, as measured by the number of active lever presses, in FSLs treated with differentiated MSC-EAAT as compared to naïve FSLs on the first testing day (day 14), and in FSLs treated with differentiated or undifferentiated cells on day 20, as compared to naïve FSLs and free GNP-treated FSLs (Figure 3c (day 1: MSC-EAAT-FSL vs. naive FSLs, $p<0.05$; MSC-EAAT FSLs vs. SD, n.s. ($p>0.05$); day 7: SD, MSC-EAAT-treated and undifferentiated MSCs-treated FSLs vs. naive FSLs and free GNP-treated FSLs: $p<0.001$).

Tracking of cell migration and final location in the brain

To dynamically track the migration route of the cells in the brain, *in vivo* CT scans were conducted in treated or control FSL rats. As early as 24 hours post-transplantation, free GNPS were more diffusely dispersed (Fig 4a), while MSC-EAAT were more directed in movement (Figure 4b), and one month post-transplantation, free GNPs were scattered and widely spread throughout the brain (Figure 4c), while the GNP-labeled MSC-EAATs migrated and concentrated in specific brain regions (Figure 4d). At one month, the FSLs were sacrificed and further examined for the exact location, distribution and final fate of GNPs via *ex-vivo* CT scans, using contrast agents and higher resolution and radiation dose (Figure 4e-f). A notable difference in spatial distribution of GNPs was observed between groups: While free GNPs were scattered and widely dispersed in both brain hemispheres, suggesting a passive diffusion motion rather than active migration (Figure 4e), GNP-conjugated MSC-EAATs clearly accumulated in a specific brain area within the left hemisphere, encompassing the left hippocampal region (Figure 4f).

To confirm the imaging results, we conducted immunohistochemical staining of brain slices from rat brains isolated at the conclusion of behavioral testing. MSC-EAAT were distinguished from rat cells using anti-human mitochondria primary antibodies and fluorescent staining, confirming presence of the human cells in the dentate gyrus of MSC-EAAT treated FSLs (Figure 4g-h).

To quantify the exact amount of cells that reached each brain region, tissues from 30 different brain regions were excised and analyzed using FAAS. The different migration patterns of free GNPs and MSC-EAATs were clearly notable. Free GNPs injected to FSLs were detected in many different regions, and mostly in the left ventricles (total of $71,975±1287*10^6$ GNPs; Figure 5a; one-way ANOVA $F(4,10)=68.16$; Tukey's post hoc: no significant difference between left and right hemisphere brain regions, $p>0.05$; left ventricle vs. all other regions, $p<0.0001$).

However, MSC-EAATs were concentrated mainly in the left dentate gyrus of the hippocampus (total of $4.72×10^4±4720$ MSC-EAATs) and ventricle ($9.38×10^4±6570$ MSC-EAATs) of FSLs (Figure 5b), and significantly lower amounts of MSC-EAATs were detected in the CA1, CA3, substantia nigra, bed nucleus of the stria terminalis, ventral tegmental area, arcuate nucleus, basolateral amygdala, central amygdala, and lateral habenula (mean of 7016±1287 MSC-EAATs, Figure 5b) (one-way ANOVA, $F(3,8)=746.4$; $p<0.0001$; Tukey's post hoc: dentate gyrus vs. all other regions $p<0.5$-0.0001).

For undifferentiated MSCs, we found that cells were mostly located in the cingulate cortex, with lower amounts in all other regions examined, including the dentate gyrus ($8.49×10^4±1.18 ×10^4$; rest of the brain: 3229±1220; one-way ANOVA, $F(2,6)=137.57$, $p<0.0001$; Tukey's post hoc, $p<0.0001$ for cingulate vs. all other areas; Figure 5c).

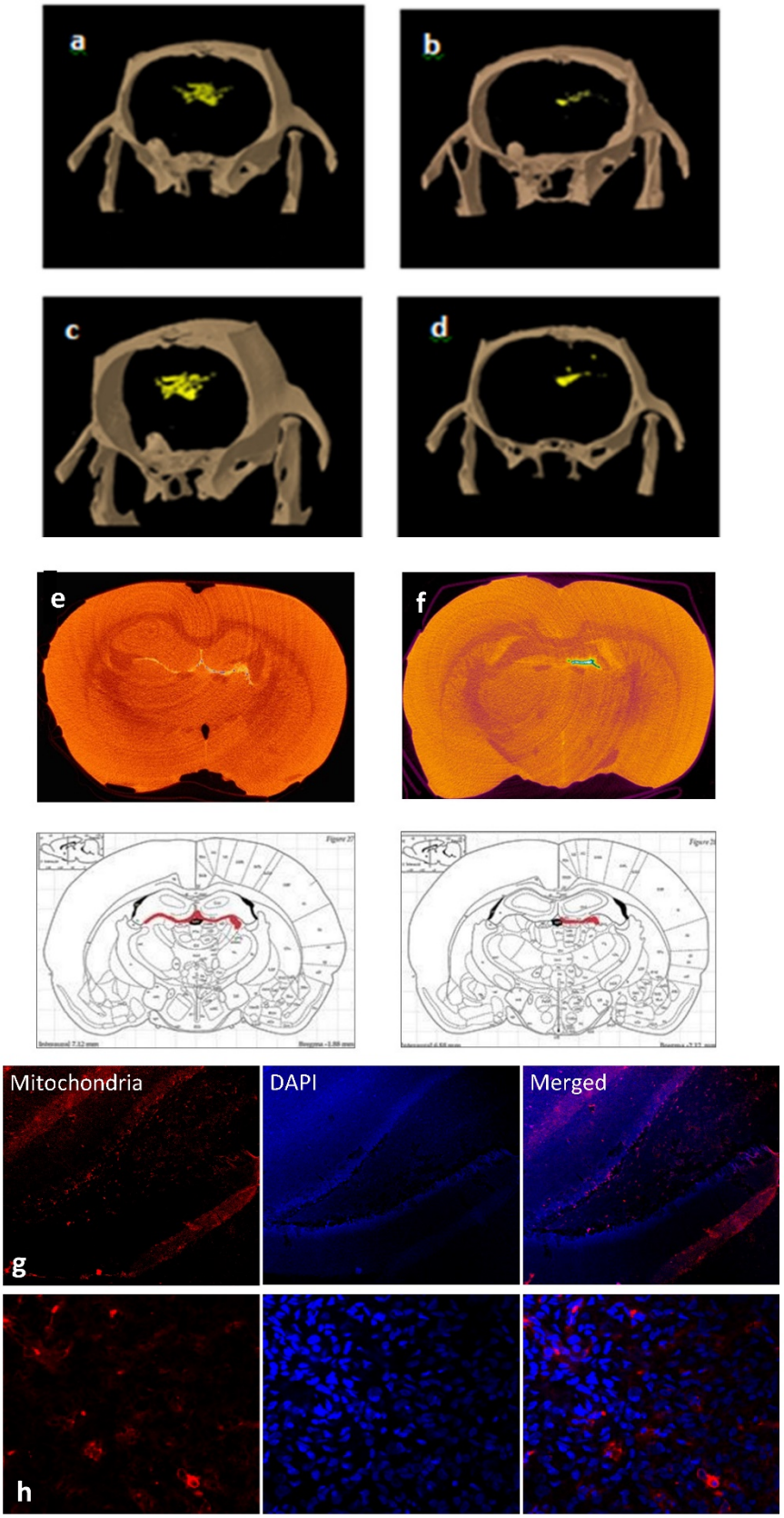

Figure 4. Tracking of MSC migration and localization within brain. a-d: Representative three-dimensional *in vivo* volume rendering micro-CT scans, (a-b) 24 hrs (a: Free GNPs, b: MSC-EAAT) and (c-d) 1 month post treatment (c: Free-GNPs, d: MSC-EAAT) (n=3 for both groups). **e-f:** *Ex-vivo* micro-CT scans. Representative *ex vivo* coronal CT images and corresponding rat brain atlas reference (Paxinos &Watson) with red color indicating GNP distribution: (e) Free GNPs, (f) MSC-EAAT. Images of free GNPs adapted with permission from [55] copyright 2014 American Chemistry society. **g-h:** Representative coronal brain slices of the dentate gyrus stained with mouse anti-human mitochondria monoclonal primary antibody (1:400), and visualized with an Alexa Fluor 568 goat anti-mouse secondary antibody (1:1000, red) as well as DAPI staining (blue): (g) ×10 magnification. (h) ×60 magnification. Fluorescent images were acquired using an Olympus confocal microscope. n=3/group.

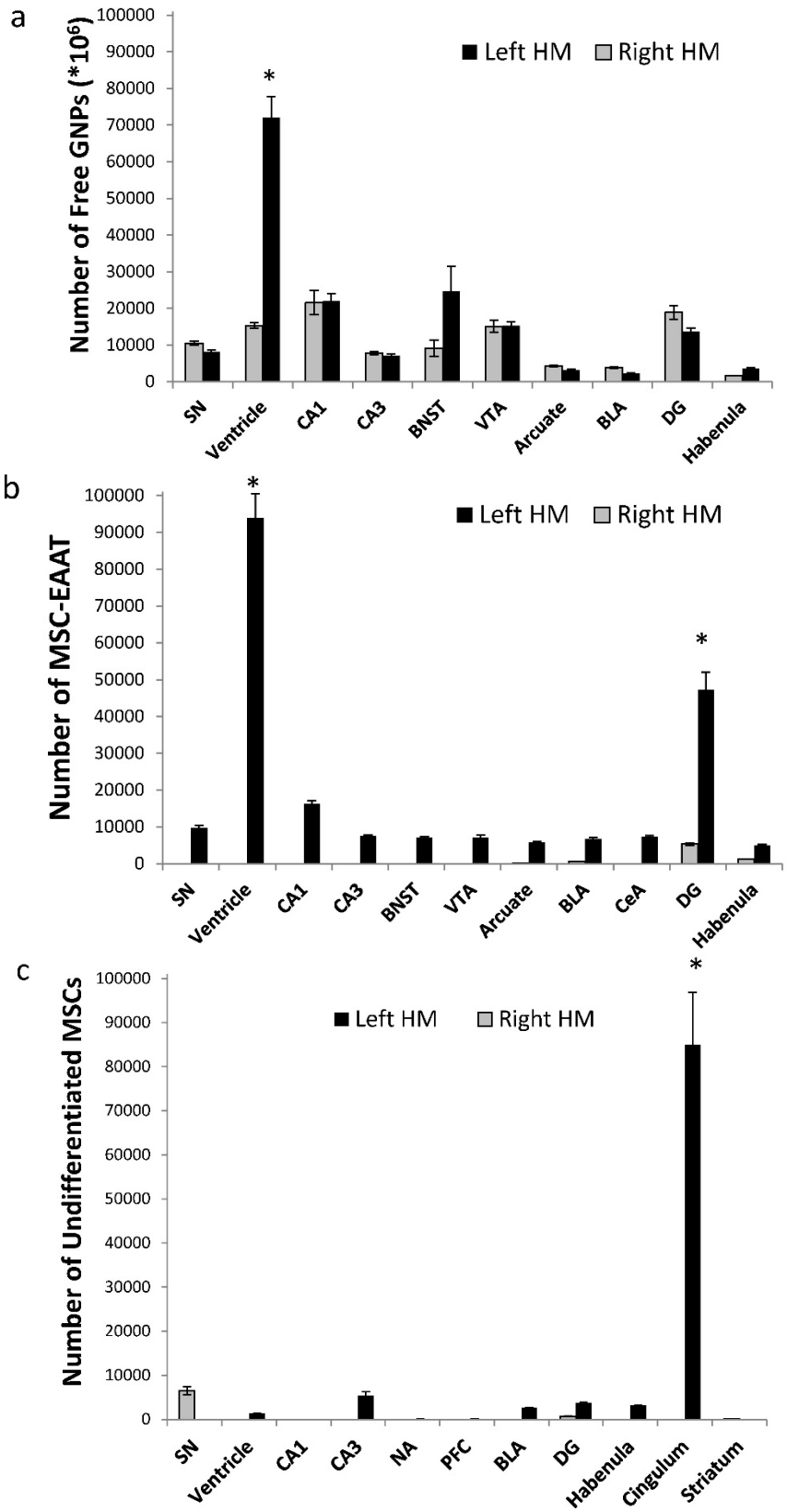

Figure 5. Amount of MSC-EAATs in brain regions. Using Flame Atomic Absorption Spectroscopy (FAAS) analysis of 15 bi-hemispheric brain punches, we determined the amount of gold in each region: (a) Free-GNPs were widely dispersed within the various brain regions. (b) MSC-EAAT: Analysis showed that the differentiated cells migrated mostly to the dentate gyrus (DG), *p<0.05. (c) Undifferentiated MSCs (uMSCs): The analysis showed that uMSCs migrated mostly to the cingulate cortex. *p<0.05 (panel c adapted with permission from [55] copyright 2014 American Chemistry society). Abbreviations: PFC, prefrontal cortex; NA, nucleus accumbens; CeA, central amygdala; BLA, basolateral amygdala; VTA, ventral tegmental area; DG, dentate gyrus; BNST, bed nucleus of stria terminalis; SN, substantia nigra; punches also taken from the lateral habenula, cingulate cortex, striatum, arcuate nucleus and verntricles. Samples were analyzed in triplicate, values presented as mean±SEM.

BDNF and EAAT1 mRNA levels in the hippocampus

Next, we examined the expression levels of EAAT in the dentate gyrus and fimbria 21 days post transplantation. We additionally examined expression levels of brain derived neurotrophic factor **(**BDNF**)**, which has a role in the etiology of major depression and is a reliable biomarker for the depressed state [67, 68]. Acute and chronic stress decreases BDNF expression levels in the hippocampus of rodents [69-71], while various types of chronic antidepressant treatments increase BDNF expression in this region [72, 73]. Using RT-qPCR, we found that both EAAT1 (Fig. 6a) and BDNF (Fig. 7a) mRNA expression levels were significantly increased in the dentate gyrus of MSC-EAAT treated FSLs as compared to undifferentiated MSC-treated FSLs and FSL controls (Figure 6a and 7a; EAAT1: one-way ANOVA: $F[2,9]=7.278$, $p=0.0132$; Newman-Keuls correction, $p<0.01$ MSC-EAAT compared to undifferentiated MSC and $p<0.05$ MCS-EAAT vs. control; BDNF: $F[2,9]=6.762$, $p=0.0161$; Newman-Keuls correction, $p<0.05$ MSC-EAAT compared to undifferentiated MSC and control). Immunohistochemical staining of the dentate gyrus and subsequent quantification of relative protein expression showed that EAAT1 protein expression levels were significantly elevated in MSC-EAAT-treated FSLs as compared to control FSLs and undifferentiated MSC-treated FSLs (Fig 6b-d; $p<0.05$; t-test). BDNF protein expression levels were significantly elevated in both MSC-EAAT-treated and undifferentiated MSC treated FSLs, as compared to control FSLs (Fig 7b-d; $p<0.05$).

Discussion

Herein, we found that human MSCs differentiated to express high levels of EAAT1 and EAAT2, administered i.c.v., had a long-term attenuating effect on depressive-like behavior in FSL rats, including motivation, novelty exploration and hedonia. Using non-invasive, real-time imaging of the GNPs that labelled the cells, followed by quantitative analysis of gold amounts in brain regions, we found that the majority of MSC-EAAT migrated to the dentate gyrus of the hippocampus, and were observed in this region up to one month post-transplantation.

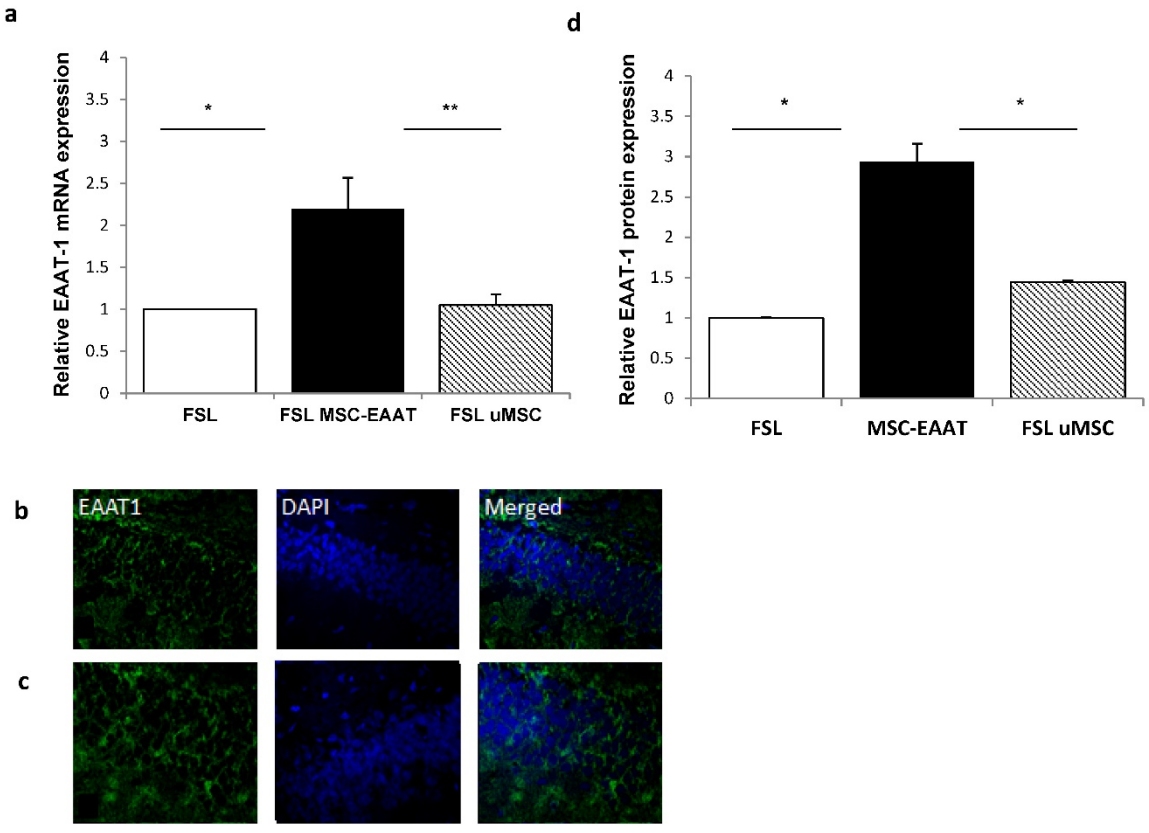

Figure 6. Hippocampal EAAT1 mRNA levels and immunofluorescence staining. a. mRNA expression levels of EAAT1 were significantly higher in FSL rats treated with MSC-EAAT as compared to control FSLs. Results expressed in arbitrary units (one way ANOVA, **p<0.01 MSC-EAAT compared to undifferentiated MSC and *p<0.05 MCS-EAAT vs. control). Values presented as mean ± SEM of 3-4 rats. **b-c:** Immunofluorescence staining for EAAT1- in (b) FSL-Control, (c) MSC-EAAT. **d)** Quantification of relative EAAT1 expression as measured by ImageJ software (mean signal value per group) showed higher protein levels in MSC-EAAT treated FSLs as compared to control FSLs and undifferentiated MSC-treated FSLs (*p<0.05). Values presented as mean + SEM.

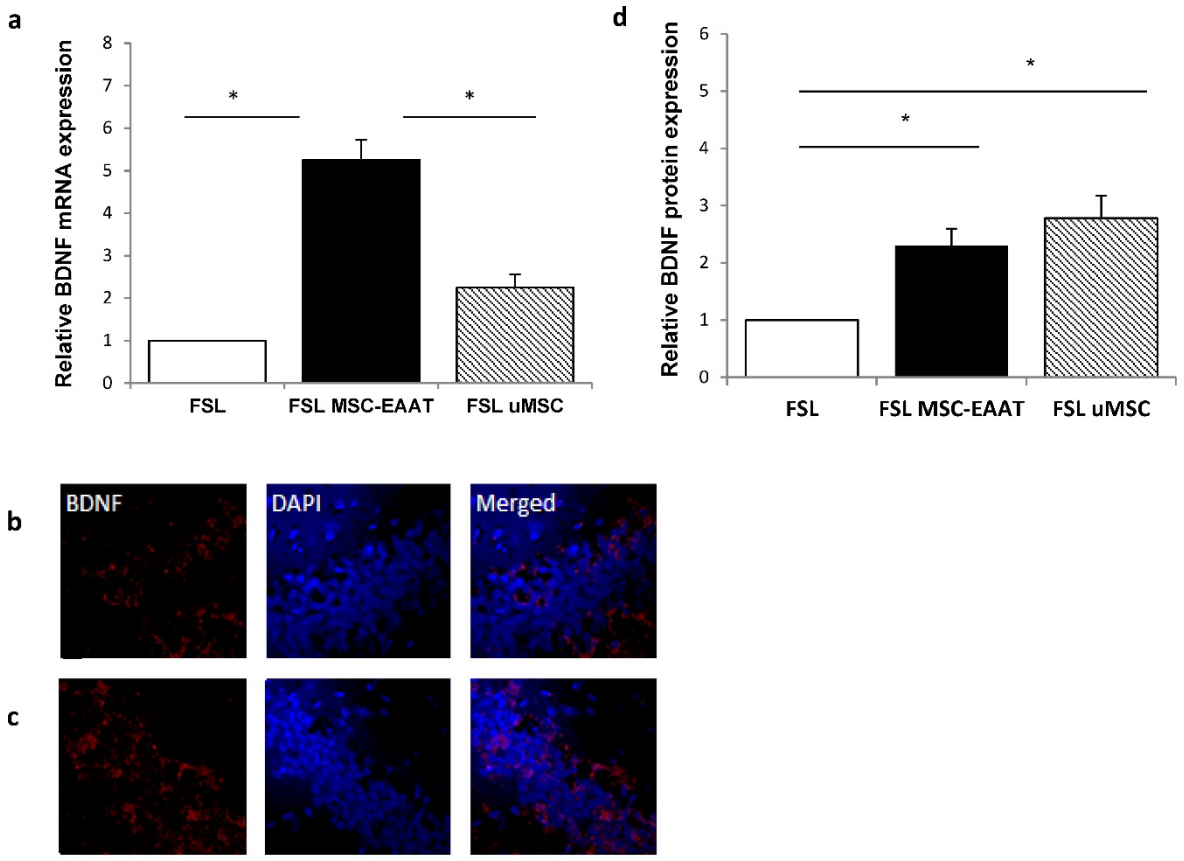

Figure 7. Hippocampal BDNF mRNA levels and immunohistochemical staining. a. mRNA expression levels of BDNF were significantly higher in FSL rats treated with MSC-EAAT as compared to control FSLs. Results are expressed in arbitrary units; presented as mean ± SEM of 3-4 rats. (one-way ANOVA, *p<0.05 MSC-EAAT vs. undifferentiated MSC and control). **b-c:** Immunofluorescent staining for BDNF in (b) FSL-Control and (c) MSC-EAAT. **d)** Quantification of relative BDNF expression as measured by ImageJ software (mean signal value per group) showed higher protein levels in MSC-EAAT treated FSLs and undifferentiated MSC-treated FSLs as compared to control FSLs (*p<0.05). Values presented as mean + SEM.

We note that the time course of the behavioral effect of MSC-EAAT on FSLs seems to be similar to that of other pharmacological and non-pharmacological anti-depressant treatments, in which the strongest effect occurs within 2-3 weeks after treatment, when a balance in expression of depression-related receptors (e.g., dopamine, 5-HT) is reached [61, 74].

Long-term elevation of EAAT-1 expression levels were found in the hippocampus of MSC-EAAT FSLs, but not in FSLs treated with undifferentiated cells. This suggests that the differentiated cells have an advantage over undifferentiated cells, in that higher EAAT1 expression led to the MSC-EAAT–induced improvement in all three depressive-like behaviors, while undifferentiated MSCs, which did not show higher EAAT1 expression, improved only one behavior. The manipulation of MSCs by the differentiation process did not affect local BDNF production, and the capacity of the cells seems to be reserved. We assume that the difference between mRNA and protein levels of BDNF in the undifferentiated MSC group is probably due to post-transcriptional regulation. The increase in BDNF expression ultimately seen in both treatment groups likely indicates an association of BDNF with the behavioral improvement that occurred in these groups (though behavior improved to a lesser extent in undifferentiated MSCs).

Our results suggest that depressive-like behaviors may, at least in part, be modulated by glutamatergic transmission, and EAAT deficiency in particular. We postulate that the MSC-EAATs that migrated to the hippocampus induced the increase in local EAAT1 and BDNF, by their production, and/or communication with native cell populations via various signaling mechanisms. Thus, MSC-EAAT treatment may have restored normal hippocampal glutamatergic transmission and BDNF levels, which ultimately improved depressive-like behaviors. This hypothesis is supported by a recent study showing dysfunctional astrocytic glutamate regulation, including downregulation of glia EAAT1 expression levels, in the hippocampus of FSLs [75].

It is notable that other recent studies have shown a beneficial effect of stem cell treatment on depression-related parameters. Treatment of rats with intravenous human bone-marrow derived MSCs

prevented anhedonia and working memory impairments induced by traumatic brain injury [76]. Combined treatment with intravenous neural stem cells and the antidepressant sertraline reduced depressive-like behaviors in rats exposed to prenatal and adolescent stress [77], and intra-hippocampal transplantation of MSCs in a rat model for depression resulted in enhanced neurogenesis in this region [78].

Changes in the hippocampus, including localized mechanisms of hippocampal neuroplasticity, are linked to depression [79]. Accumulating evidence suggests that chronic stress and major depression are associated with hippocampal volume reductions specific to the dentate gyrus [80], and structural changes including loss of dendritic spines and synapses, reduced dendritic arborization, and diminished glial cells in the hippocampus [81]. Such alterations are thought to contribute to various behavioral symptoms of depression, including disruption of cognition, mood, emotion, motivation, and reward [82]. Neurotrophic factors and central monoamines are associated with alterations in hippocampal progenitor proliferation and cell survival, an effect which is reversed by antidepressants via stimulation of neurotrophic factors, including BDNF, which regulates synaptic protein synthesis, and by modulation of glial cells, causing an increase in dendritic arborization and synaptogenesis [81]. Astrocytes are potent regulators of synaptic plasticity, and astrocyte-mediated metaplasticity mechanisms may be engaged by pathological signaling in the hippocampus [83]. Small packets of glutamate are released by astrocytes, acting on extrasynaptic glutamate NMDA receptor subtype 2B [84-87]. Activation of a single astrocyte in the CA1 triggers synchronous slow inward currents in numerous adjacent neurons, suggesting that astrocytes play a role in coordination of neural synchrony [83, 86]. Taken together, we postulate that MSC-EAATs that migrated to the hippocampus integrated in this region and became part of the tissue machinery, thus increasing hippocampal EAAT and BDNF levels. This may have provided an effective combination of buffering of extracellular glutamate levels, together with increased neurotrophic support, leading to regeneration and recovery in the tissue, and ultimately, to a prolonged beneficial effect on depressive manifestations in FSL rats. Future research may elucidate additional cross-talk between MSC-EAATs and the host brain tissue.

Moreover, we note that although most cells reached the dentate gyrus of the hippocampus, they were also dispersed in other emotion-associated regions. While the cells were engrafted in these sites in much lower amounts, they may have also contributed to the beneficial effect of MSC-EAATs on depressive-like behavior.

In addition, substantial amounts of undifferentiated MSCs were engrafted in the cingulate cortex, with significantly smaller amounts in all other regions, including the dentate gyrus. The cingulate cortex is connected to reward and hedonia [88], which may have affected the hedonic-like response in FSLs without regulation by EAAT1. However, the effect of these cells on the hedonic-like response occurred only at the later timepoint. Moreover, undifferentiated MSCs did not affect novelty exploration (as compared to FSL controls and SD), or immobility in the swim test. Future studies should examine whether a combination of differentiated and undifferentiated MSCs could provide an additive beneficial effect on depressive-like behavior.

In conclusion, our findings imply that treatment with novel MSC-EAAT may induce both neurotrophic and glutamatergic neurotransmission changes within the hippocampus, ultimately leading to improvement in depressive-like behavior. Thus, differentiation of MSCs to express EAAT can offer an added value to the inherent properties of MSCs, and enhance stem-cell based treatment of depression.

Moreover, our technique for cell labeling with GNPs for non-invasive, real-time and longitudinal imaging and tracking of stem cells can answer the challenges that exist particularly within deep brain structures that are difficult to access, if not completely inaccessible. By providing quantitative information on the cells, this technique has the potential to elucidate poorly-understood mechanisms affecting the outcome of cell therapy for brain disorders, concurrently with elucidation of processes underlying the beneficial effect of these cells on depressive behavior.

Acknowledgement

We wish to thank Dr. Tamar Sadan for critical editing of the manuscript. This work was partially supported by the Ministry of Science, Technology & Space doctoral scholarship to O. Betzer.

Supplementary Material

Supplementary methods.
http://www.thno.org/v07p2690s1.pdf

Competing Interests

The authors have declared that no competing interest exists.

References

1. Kessler RC, Berglund P, Demler O, Jin R, Koretz D, Merikangas KR, et al. The epidemiology of major depressive disorder: results from the National Comorbidity Survey Replication (NCS-R). JAMA. 2003; 289: 3095-105.
2. Mathews DC, Henter ID, Zarate CA. Targeting the glutamatergic system to treat major depressive disorder: rationale and progress to date. Drugs. 2012; 72: 1313-33.
3. Mauri MC, Ferrara A, Boscati L, Bravin S, Zamberlan F, Alecci M, et al. Plasma and platelet amino acid concentrations in patients affected by major depression and under fluvoxamine treatment. Neuropsychobiology. 1998; 37: 124-9.
4. Kim JS, Schmid-Burgk W, Claus D, Kornhuber HH. Increased serum glutamate in depressed patients. Arch Psychiatr Nervenkr. 1982; 232: 299-304.
5. Mitani H, Shirayama Y, Yamada T, Maeda K, Ashby CR, Jr., Kawahara R. Correlation between plasma levels of glutamate, alanine and serine with severity of depression. Prog Neuropsychopharmacol Biol Psychiatry. 2006; 30: 1155-8.
6. Frye MA, Tsai GE, Huggins T, Coyle JT, Post RM. Low cerebrospinal fluid glutamate and glycine in refractory affective disorder. Biol Psychiatry. 2007; 61: 162-6.
7. Francis PT, Poynton A, Lowe SL, Najlerahim A, Bridges PK, Bartlett JR, et al. Brain amino acid concentrations and Ca2+-dependent release in intractable depression assessed antemortem. Brain Res. 1989; 494: 315-24.
8. Nowak G, Ordway GA, Paul IA. Alterations in the N-methyl-D-aspartate (NMDA) receptor complex in the frontal cortex of suicide victims. Brain Res. 1995; 675: 157-64.
9. Holemans S, De Paermentier F, Horton RW, Crompton MR, Katona CL, Maloteaux JM. NMDA glutamatergic receptors, labelled with [3H]MK-801, in brain samples from drug-free depressed suicides. Brain Res. 1993; 616: 138-43.
10. Hascup KN, Hascup ER, Stephens ML, Glaser PE, Yoshitake T, Mathe AA, et al. Resting glutamate levels and rapid glutamate transients in the prefrontal cortex of the Flinders Sensitive Line rat: a genetic rodent model of depression. Neuropsychopharmacology. 2011; 36: 176977.
11. Matrisciano F, Caruso A, Orlando R, Marchiafava M, Bruno V, Battaglia G, et al. Defective group-II metaboropic glutamate receptors in the hippocampus of spontaneously depressed rats. Neuropharmacology. 2008; 55: 525-31.
12. Kovacevic T, Skelin I, Minuzzi L, Rosa-Neto P, Diksic M. Reduced metabotropic glutamate receptor 5 in the Flinders Sensitive Line of rats, an animal model of depression: an autoradiographic study. Brain Res Bull. 2012; 87: 406-12.
13. Ryan B, Musazzi L, Mallei A, Tardito D, Gruber SH, El Khoury A, et al. Remodelling by early-life stress of NMDA receptor-dependent synaptic plasticity in a gene-environment rat model of depression. Int J Neuropsychopharmacol. 2009; 12: 553-9.
14. Ongur D, Drevets WC, Price JL. Glial reduction in the subgenual prefrontal cortex in mood disorders. Proc Natl Acad Sci USA. 1998; 95: 13290-5.
15. Rajkowska G, Miguel-Hidalgo JJ, Wei J, Dilley G, Pittman SD, Meltzer HY, et al. Morphometric evidence for neuronal and glial prefrontal cell pathology in major depression. Biol Psychiatry. 1999; 45: 1085-98.
16. Cotter DR, Pariante CM, Everall IP. Glial cell abnormalities in major psychiatric disorders: the evidence and implications. Brain Res Bull. 2001; 55: 585-95.
17. Cotter D, Mackay D, Chana G, Beasley C, Landau S, Everall IP. Reduced neuronal size and glial cell density in area 9 of the dorsolateral prefrontal cortex in subjects with major depressive disorder. Cereb Cortex. 2002; 12: 386-94.
18. Uranova NA, Vostrikov VM, Orlovskaya DD, Rachmanova VI. Oligodendroglial density in the prefrontal cortex in schizophrenia and mood disorders: a study from the Stanley Neuropathology Consortium. Schizophr Res. 2004; 67: 269-75.
19. Pittenger C, Duman RS. Stress, depression, and neuroplasticity: a convergence of mechanisms. Neuropsychopharmacology. 2008; 33: 88-109.
20. Choudary PV, Molnar M, Evans SJ, Tomita H, Li JZ, Vawter MP, et al. Altered cortical glutamatergic and GABAergic signal transmission with glial involvement in depression. Proc Natl Acad Sci USA. 2005; 102: 15653-8.
21. Bernard R, Kerman IA, Thompson RC, Jones EG, Bunney WE, Barchas JD, et al. Altered expression of glutamate signaling, growth factor, and glia genes in the locus coeruleus of patients with major depression. Mol Psychiatry. 2011; 16: 634-46.
22. Lee LJ, Lo FS, Erzurumlu RS. NMDA receptor-dependent regulation of axonal and dendritic branching. J Neurosci. 2005; 25: 2304-11.
23. Gorman JM, Docherty JP. A hypothesized role for dendritic remodeling in the etiology of mood and anxiety disorders. J Neuropsychiatry Clin Neurosci. 2010; 22: 256-64.
24. Bessa JM, Ferreira D, Melo I, Marques F, Cerqueira JJ, Palha JA, et al. The mood-improving actions of antidepressants do not depend on neurogenesis but are associated with neuronal remodeling. Mol Psychiatry. 2009; 14: 764-73, 39.
25. Machado-Vieira R, Ibrahim L, Henter ID, Zarate CA, Jr. Novel glutamatergic agents for major depressive disorder and bipolar disorder. Pharmacol Biochem Behav. 2012; 100: 678-87.
26. Yang C, Hu YM, Zhou ZQ, Zhang GF, Yang JJ. Acute administration of ketamine in rats increases hippocampal BDNF and mTOR levels during forced swimming test. Ups J Med Sci. 2013; 118: 3-8.
27. Li N, Liu RJ, Dwyer JM, Banasr M, Lee B, Son H, et al. Glutamate N-methyl-D-aspartate receptor antagonists rapidly reverse behavioral and synaptic deficits caused by chronic stress exposure. Biol Psychiatry. 2011; 69: 754-61.
28. Yang C, Hong T, Shen J, Ding J, Dai XW, Zhou ZQ, et al. Ketamine exerts antidepressant effects and reduces IL-1beta and IL-6 levels in rat prefrontal cortex and hippocampus. Exp Ther Med. 2012; 5: 1093-6.
29. Wang J, Goffer Y, Xu D, Tukey DS, Shamir DB, Eberle SE, et al. A single subanesthetic dose of ketamine relieves depression-like behaviors induced by neuropathic pain in rats. Anesthesiology. 2011; 115: 812-21.
30. Zarate CA, Jr., Singh JB, Carlson PJ, Brutsche NE, Ameli R, Luckenbaugh DA, et al. A randomized trial of an N-methyl-D-aspartate antagonist in treatment-resistant major depression. Arch Gen Psychiatry. 2006; 63: 856-64.
31. Thase ME, Haight BR, Richard N, Rockett CB, Mitton M, Modell JG, et al. Remission rates following antidepressant therapy with bupropion or selective serotonin reuptake inhibitors: a meta-analysis of original data from 7 randomized controlled trials. J Clin Psychiatry. 2005; 66: 974-81.
32. Nitkin CR, Bonfield TL. Concise Review: Mesenchymal Stem Cell Therapy for Pediatric Disease: Perspectives on Success and Potential Improvements. Stem Cells Transl Med. 2016; 6(2): 539-565.
33. Squillaro T, Peluso G, Galderisi U. Clinical Trials With Mesenchymal Stem Cells: An Update. Cell Transplant. 2016; 25: 829-48.
34. Trounson A, McDonald C. Stem cell therapies in clinical trials: Progress and challenges. Cell Stem Cell. 2015; 17: 11-22.
35. Uccelli A, Laroni A, Freedman MS. Mesenchymal stem cells for the treatment of multiple sclerosis and other neurological diseases. Lancet Neurol. 2011; 10: 649-56.
36. Trounson A, Thakar RG, Lomax G, Gibbons D. Clinical trials for stem cell therapies. BMC Med. 2011; 9: 52.
37. Uys JD, Reissner KJ. Glutamatergic neuroplasticity in cocaine addiction. Prog Mol Biol Transl Sci. 2011; 98: 367-400.
38. Spaeth E, Klopp A, Dembinski J, Andreeff M, Marini F. Inflammation and tumor microenvironments: defining the migratory itinerary of mesenchymal stem cells. Gene Ther. 2008; 15: 730-8.
39. Joyce N, Annett G, Wirthlin L, Olson S, Bauer G, Nolta JA. Mesenchymal stem cells for the treatment of neurodegenerative disease. Regen Med. 2010; 5: 933-46.
40. Meirelles Lda S, Fontes AM, Covas DT, Caplan AI. Mechanisms involved in the therapeutic properties of mesenchymal stem cells. Cytokine Growth Factor Rev. 2009; 20: 419-27.
41. Crigler L, Robey RC, Asawachaicharn A, Gaupp D, Phinney DG. Human mesenchymal stem cell subpopulations express a variety of neuro-regulatory molecules and promote neuronal cell survival and neuritogenesis. Exp Neurol. 2006; 198: 54-64.
42. Ricles LM, Nam SY, Sokolov K, Emelianov SY, Suggs LJ. Function of mesenchymal stem cells following loading of gold nanotracers. Int J Nanomedicine. 2011; 6: 407-16.
43. Tantrawatpan C, Manochantr S, Kheolamai P, Y UP, Supokawej A, Issaragrisil S. Pluripotent gene expression in mesenchymal stem cells from human umbilical cord Wharton's jelly and their differentiation potential to neural-like cells. J Med Assoc Thai. 2013; 96: 1208-17.
44. Villa C, Erratico S, Razini P, Fiori F, Rustichelli F, Torrente Y, et al. Stem cell tracking by nanotechnologies. Int J Mol Sci. 2010; 11: 1070-81.
45. Nguyen PK, Riegler J, Wu JC. Stem cell imaging: from bench to bedside. Cell Stem Cell. 2014; 14: 431-44.
46. Frangioni JV, Hajjar RJ. In vivo tracking of stem cells for clinical trials in cardiovascular disease. Circulation. 2004; 110: 3378-83.
47. Xu C, Zhao W. Nanoparticle-based Monitoring of Stem Cell Therapy. Theranostics. 2013; 3: 616-7.
48. Phinney DG, Prockop DJ. Concise review: mesenchymal stem/multipotent stromal cells: the state of transdifferentiation and modes of tissue repair--current views. Stem Cells. 2007; 25: 2896-902.
49. Shihabuddin LS, Aubert I. Stem cell transplantation for neurometabolic and neurodegenerative diseases. Neuropharmacology. 2010; 58: 845-54.
50. Karp JM, Leng Teo GS. Mesenchymal stem cell homing: the devil is in the details. Cell Stem Cell. 2009; 4: 206-16.
51. Ankrum J, Karp JM. Mesenchymal stem cell therapy: Two steps forward, one step back. Trends Mol Med. 2010; 16: 203-9.
52. Arvizo R, Bhattacharya R, Mukherjee P. Gold nanoparticles: opportunities and challenges in nanomedicine. Expert Opin Drug Deliv. 2010; 7: 753-63.
53. Mieszawska AJ, Mulder WJ, Fayad ZA, Cormode DP. Multifunctional gold nanoparticles for diagnosis and therapy of disease. Mol Pharm. 2013; 10: 831-47.
54. Betzer O, Meir R, Dreifuss T, Shamalov K, Motiei M, Shwartz A, et al. In-vitro Optimization of Nanoparticle-Cell Labeling Protocols for In-vivo Cell Tracking Applications. Sci Rep. 2015; 5: 15400.
55. Betzer O, Shwartz A, Motiei M, Kazimirsky G, Gispan I, Damti E, et al. Nanoparticle-based CT imaging technique for longitudinal and quantitative stem cell tracking within the brain: application in neuropsychiatric disorders. ACS Nano. 2014; 8: 9274-85.
56. Popovtzer R, Agrawal A, Kotov NA, Popovtzer A, Balter J, Carey TE, et al. Targeted gold nanoparticles enable molecular CT imaging of cancer. Nano Lett. 2008; 8: 4593-6.
57. Kalivas PW, Volkow ND. New medications for drug addiction hiding in glutamatergic neuroplasticity. Mol Psychiatry. 2011; 16: 974-86.

58. Roberts-Wolfe DJ, Kalivas PW. Glutamate Transporter GLT-1 as a Therapeutic Target for Substance Use Disorders. CNS Neurol Disord Drug Targets. 2015; 14: 745-56.
59. Kazlauckas V, Schuh J, Dall'Igna OP, Pereira GS, Bonan CD, Lara DR. Behavioral and cognitive profile of mice with high and low exploratory phenotypes. BehavBrain Res. 2005; 162: 272-8.
60. Strekalova T, Spanagel R, Bartsch D, Henn FA, Gass P. Stress-induced anhedonia in mice is associated with deficits in forced swimming and exploration. Neuropsychopharmacology. 2004; 29: 2007-17.
61. Friedman A, Frankel M, Flaumenhaft Y, Merenlender A, Pinhasov A, Feder Y, et al. Programmed acute electrical stimulation of ventral tegmental area alleviates depressive-like behavior. Neuropsychopharmacology. 2009; 34: 1057-66.
62. De La GR, Asnis GM, Fabrizio KR, Pedrosa E. Acute diclofenac treatment attenuates lipopolysaccharide-induced alterations to basic reward behavior and HPA axis activation in rats. Psychopharmacology (Berl). 2005; 179: 356-65.
63. De La GR, Fabrizio KR, Radoi GE, Vlad T, Asnis GM. The non-steroidal anti-inflammatory drug diclofenac sodium attenuates lipopolysaccharide-induced alterations to reward behavior and corticosterone release. BehavBrain Res. 2004; 149: 77-85.
64. de Crespigny A, Bou-Reslan H, Nishimura MC, Phillips H, Carano RA, D'Arceuil HE. 3D micro-CT imaging of the postmortem brain. J Neurosci Methods. 2008; 171: 207-13.
65. Saito S, Mori Y, Yoshioka Y, Murase K. High-resolution ex vivo imaging in mouse spinal cord using micro-CT with 11.7T-MRI and myelin staining validation. Neurosci Res. 2012; 73: 337-40.
66. Brachman RA, McGowan JC, Perusini JN, Lim SC, Pham TH, Faye C, et al. Ketamine as a prophylactic against stress-induced depressive-like behavior. Biol Psychiatry. 2016; 79: 776-86.
67. Bjorkholm C, Monteggia LM. BDNF - a key transducer of antidepressant effects. Neuropharmacology. 2015; 102: 72-9.
68. Allen AP, Naughton M, Dowling J, Walsh A, Ismail F, Shorten G, et al. Serum BDNF as a peripheral biomarker of treatment-resistant depression and the rapid antidepressant response: A comparison of ketamine and ECT. J Affect Disord. 2015; 186: 306-11.
69. Smith MA, Makino S, Kvetnansky R, Post RM. Stress and glucocorticoids affect the expression of brain-derived neurotrophic factor and neurotrophin-3 mRNAs in the hippocampus. J Neurosci. 1995; 15: 1768-77.
70. Li G, Wang Y, Yan M, Ma H, Gao Y, Li Z, et al. Time-dependent co-relation of BDNF and CREB mRNAs in adult rat brains following acute psychological stress in the communication box paradigm. Neurosci Lett. 2016; 624: 34-41.
71. Morozova A, Zubkov E, Strekalova T, Kekelidze Z, Storozeva Z, Schroeter CA, et al. Ultrasound of alternating frequencies and variable emotional impact evokes depressive syndrome in mice and rats. Prog Neuropsychopharmacol Biol Psychiatry. 2016; 68: 52-63.
72. Nibuya M, Morinobu S, Duman RS. Regulation of BDNF and trkB mRNA in rat brain by chronic electroconvulsive seizure and antidepressant drug treatments. J Neurosci. 1995; 15: 7539-47.
73. Su Q, Tao W, Huang H, Du Y, Chu X, Chen G. Protective effect of liquiritigenin on depressive-like behavior in mice after lipopolysaccharide administration. Psychiatry Res. 2016; 240: 131-6.
74. Zangen A, Overstreet DH, Yadid G. Increased catecholamine levels in specific brain regions of a rat model of depression: normalization by chronic antidepressant treatment. Brain Res. 1999; 824: 243-50.
75. Gomez-Galan M, De Bundel D, Van Eeckhaut A, Smolders I, Lindskog M. Dysfunctional astrocytic regulation of glutamate transmission in a rat model of depression. Mol Psychiatry. 2013; 18: 582-94.
76. Darkazalli A, Ismail AA, Abad N, Grant SC, Levenson CW. Use of human mesenchymal stem cell treatment to prevent anhedonia in a rat model of traumatic brain injury. Restor Neurol Neurosci. 2016; 34: 433-41.
77. Kigawa Y, Hashimoto E, Ukai W, Ishii T, Furuse K, Tsujino H, et al. Stem cell therapy: a new approach to the treatment of refractory depression. J Neural Transm (Vienna). 2014; 121: 1221-32.
78. Coquery N, Blesch A, Stroh A, Fernandez-Klett F, Klein J, Winter C, et al. Intrahippocampal transplantation of mesenchymal stromal cells promotes neuroplasticity. Cytotherapy. 2012; 14: 1041-53.
79. MacQueen G, Frodl T. The hippocampus in major depression: evidence for the convergence of the bench and bedside in psychiatric research? Mol Psychiatry. 2011; 16: 252-64.
80. Malykhin NV, Coupland NJ. Hippocampal neuroplasticity in major depressive disorder. Neuroscience. 2015; 309: 200-13.
81. Serafini G, Hayley S, Pompili M, Dwivedi Y, Brahmachari G, Girardi P, et al. Hippocampal neurogenesis, neurotrophic factors and depression: possible therapeutic targets? CNS Neurol Disord Drug Targets. 2014; 13: 1708-21.
82. Duman CH, Duman RS. Spine synapse remodeling in the pathophysiology and treatment of depression. Neurosci Lett. 2015; 601: 20-9.
83. Jones OD. Astrocyte-mediated metaplasticity in the hippocampus: Help or hindrance? Neuroscience. 2015; 309: 113-24.
84. Araque A, Sanzgiri RP, Parpura V, Haydon PG. Calcium elevation in astrocytes causes an NMDA receptor-dependent increase in the frequency of miniature synaptic currents in cultured hippocampal neurons. J Neurosci. 1998; 18: 6822-9.
85. Boess F, Ndikum-Moffor FM, Boelsterli UA, Roberts SM. Effects of cocaine and its oxidative metabolites on mitochondrial respiration and generation of reactive oxygen species. Biochem Pharmacol. 2000; 60: 615-23.
86. Fellin T, Pascual O, Gobbo S, Pozzan T, Haydon PG, Carmignoto G. Neuronal synchrony mediated by astrocytic glutamate through activation of extrasynaptic NMDA receptors. Neuron. 2004; 43: 729-43.
87. Fellin T, Carmignoto G. Neurone-to-astrocyte signalling in the brain represents a distinct multifunctional unit. J Physiol. 2004; 559: 3-15.
88. Berridge KC, Kringelbach ML. Building a neuroscience of pleasure and well-being. Psychol Well Being. 2011; 1: 1-3.